THE JOURNAL OF PHYSICAL CHEMISTRY B

Article

pubs.acs.org/JPCB

Imaging Individual Proton-Conducting Spots on Sulfonated Multiblock-Copolymer Membrane under Controlled Hydrogen Atmosphere by Current-Sensing Atomic Force Microscopy

Masanori Hara,[†] Daiki Hattori,[‡] Junji Inukai,*[,†] Byungchan Bae,[†,¶] Takayuki Hoshi,[‡] Masaya Hara,[‡] Kenji Miyatake,[†,§] and Masahiro Watanabe*[,†]

[†]Fuel Cell Nanomaterials Center, University of Yamanashi, 6-43 Miyamae, Kofu, Yamanashi 400-0021, Japan

[‡]Interdisciplinary Graduate School of Medicine and Engineering, University of Yamanashi, 4 Takeda, Kofu, Yamanashi 400-8510, Japan

[§]Clean Energy Research Center, University of Yamanashi, 4 Takeda, Kofu, Yamanashi 400-8510, Japan

Supporting Information

ABSTRACT: The proton-conductive spots on the membrane surface of sulfonated poly(arylene ether) multiblock copolymer were successfully imaged by current-sensing atomic force microscopy under hydrogen atmosphere at various temperatures and humidities. These spots should be connected to the proton-conductive paths inside the membrane. The average diameter of the spots was approximately 12 nm, consistent with the size of hydrophilic domains observed by transmission electron microscopy. The size of the proton-conducting spots was almost unchanged regardless of the temperature and humidity, whereas the number of the spots increased at higher humidity; the total area of the proton-conducting spots increased accordingly on the membrane surface. This increase in the conducting area at high humidity should be related to the bulk ionic conductivity measured by impedance spectroscopy.

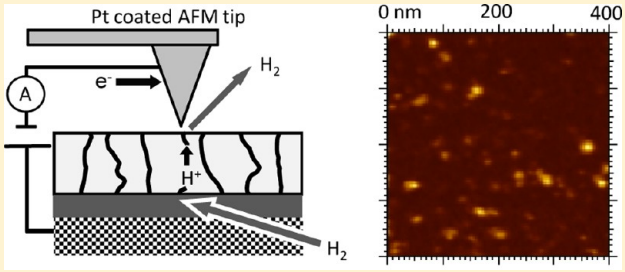

1. INTRODUCTION

Polymer electrolyte fuel cell (PEFC) attracts considerable attention as a promising alternative source of clean power for stationary, automotive, and mobile applications due to its advantage of high efficiency and low emission. Proton exchange membrane (PEM) is one of the key components that govern the cell performance of a PEFC. A wide range of characteristic properties are required for PEMs, such as thermal stability, high ionic conductivity at low humidity, and elongated lifetime, to achieve further improvements in the cell performance and durability, as well as reduction of the cost.[1−3] Perfluorosulfonic acid ionomers (PFSA), such as Nafion, are the most commonly used polymer electrolytes as commercially available PEMs, due to their high proton conductivity and chemical stability. However, their performances decrease at high temperatures above approximately 100 °C (glass transition temperature). The environmental inadaptability as well as high production cost is another problem. In recent years, membranes with sulfonated aromatic hydrocarbon (HC) structure have been extensively studied as an alternative to PFSA from the viewpoints of cost, environmental friendliness, and stability at high temperatures.[4−18] The HC-type membranes have already demonstrated promising results.[19−22]

Recently, our group has reported a series of sulfonated poly(arylene ether sulfone) (SPE) multiblock copolymers with high proton conductivity, comparable to that of Nafion, at high temperature and humidity.[23−26] The SPE block copolymer membranes showed a unique hydrophilic/hydrophobic phase-separated morphology due to the accumulated sulfonic acid groups in the hydrophilic component. These phase-separated structures resulted in interconnected ionic pathway and enhanced proton transport in the membrane. The performance of the fuel cell composed with SPEs was comparable to that obtained with the Nafion membrane at high humidity.[27,28] However, further improvement of the proton conductivity at low humidity has been an important issue, especially for automotive application. The major reasons for the conductivity drop of HC-type membranes at low humidity have been considered as ionic clusters still less developed inside HC-type membranes than PFSAs and the lower acidity of aromatic sulfonic acid groups in HC-type membranes showing lower K_a.

For the development of HC-PEMs with higher proton conductivity at low humidity, the understanding of proton transport behavior and distribution of proton-conductive paths inside the electrolyte membrane is important. The phase-separated structure of a hydrated Nafion is reported to form spontaneously from spherically shaped hydrophilic clusters, which are composed from sulfonic groups combined with water

Received: December 6, 2012
Revised: February 3, 2013
Published: March 13, 2013

molecules;[29] the hydrophilic clusters are interconnected by narrow ionic channels and form a proton-conductive network in hydrophilic fluorocarbon matrix. A recent study of small-angle X-ray scattering suggests that arrays of oriented ionic channels were embedded in a polymer matrix in the Nafion membrane.[30] We have reported that the SPE multiblock copolymers also had a well-ordered hydrophilic/hydrophobic phase-separated structure and that the sizes of hydrophilic and hydrophobic clusters were larger than that of Nafion.[24−26] The hydrophilic clusters stained with lead or silver ions in PEMs have been observed by scanning transmission electron microscopy (STEM) to obtain the phase-separated morphologies.[24−26] In spite of those important findings, it should be mentioned that those phase-separated morphologies do not directly represent the proton conduction paths inside the electrolyte membranes. Recently, for the direct observation of the proton-conductive areas on the membrane surface, atomic force microscopy (AFM) was applied with using its tip apex for current sensing at the surface to simultaneously observe the surface morphology and the proton conduction areas.[31−46] This current-sensing AFM (CS-AFM) technique has been used on Nafion[32−44] as well as HC-based membranes.[45,46] Several groups reported that the distribution of the proton-conductive domains was correlated to the hydration level of the membranes.[35,37,40,42,43]

It should be mentioned that, in almost all previous studies, the conducting protons were produced by water electrolysis, and that the high overpotential at the anodic reaction (approximately 1−2 V, which is higher than for the actual operating condition of a PEFC) was needed. The AFM measurement with water electrolysis reaction might disturb proton conduction channels due to consumption of water and production of O_2 gas at the membrane during the formation of protons. Furthermore, the large overpotential may cause a local heating of proton-conducting paths with a large drawing current. The effects of the AFM measurements on the Nafion membrane have been discussed in a previous paper.[44] In order to prepare moderate, adequate, and stable conditions for the measurement, we constructed an environment-controlling chamber for the CS-AFM measurements, which enabled us to prepare a hydrogen atmosphere at various temperatures and humidities. In this system, similar to a conventional PEFC, protons were formed by the hydrogen oxidation reaction on a gas-diffusion electrode (GDE) at the anode and transferred to the cathode through the membrane. With use of this method, the surface morphologies and the proton-conductive spots on an SPE membrane were simultaneously investigated under conditions closer to those under the practical fuel cell operation.

2. EXPERIMENTAL SECTION

2.1. Preparation of a Membrane-Electrode Assembly. GDEs with a three-layer structure, i.e., catalyst layer (CL)/microporous layer (MPL)/wet-proof carbon paper (CP), were prepared as in our previous papers.[47,48] Briefly, a paste of Pt catalyst supported on carbon black (TEC10E50E, 47.9 mass % Pt, Tanaka Kikinzoku Kogyo K.K.) containing Nafion ionomers (ion exchange capacity (IEC) = 0.9 mequiv g^{-1}, DE521, E.I. Du Pont de Nemours & Co., Inc.) as a binder, with a Nafion mass (dry basis) to carbon black ratio adjusted to 0.7, was uniformly coated on a gas diffusion layer (GDL), by use of a pulse-swirl-spray apparatus (PSS, Nordson Co., Ltd.), and then dried at 60 °C under vacuum. The Pt loadings of all electrodes were 0.5 ± 0.1 mg cm^{-2}.[49]

The membrane−electrode assemblies (MEAs) for the CS-AFM measurements were prepared by hot pressing a Nafion-coated SPE-bl-1, a sulfonated poly(arylene ether) multiblock copolymer, synthesized in our lab[23,24] with a GDE at 140 °C and 1.0 MPa for 3 min. The thickness of Nafion coated on the air-exposed side of an SPE-bl-1 membrane previously cast on a flat poly(ethylene terephthalate) sheet[23,24] was approximately 2 μm, which improved the adhesion of SPE-bl-1 to the GDE.[47] The SPE-bl-1 hot-pressed on the GDE was placed on a temperature-controlled sample stage of the system.

The gravimetric IEC of the membranes was 1.70 mequiv g^{-1}, and the numbers of repeating unit in the hydrophobic (X) and hydrophilic (Y) blocks were $X = 30$ and $Y = 8$, respectively. Characterizations of the membrane, such as titration, STEM measurements, water uptake, and proton conductivity, were carried out as previously reported.[23−26] For the STEM observations, the membrane samples were stained with lead ions by ion exchange of the sulfonic acid groups in a 0.5 M lead acetate aqueous solution, rinsed with deionized water, and dried in a vacuum oven for 12 h.

2.2. CS-AFM Measurements. A schematic illustration of the principle of the CS-AFM measurements, carried out in the environment-controlling chamber, is presented in Figure 1. A bias voltage (around 0.6 V) was applied between the AFM tip (a conductive silicon tip coated with Pt−Ir (Nanoworld)) and the GDE surface. During the dc polarization, a 5% H_2 (N_2 balance) gas was supplied to the environmental chamber (dead volume = 500 mL) at 100 mL min^{-1} and oxidized to protons on the GDE. The protons generated at the GDE are transported through the PEM and reduced to form hydrogen at the AFM tip. Only the substrate-adhering side of the membranes[23,24] was used for the tip scan and current sensing. The CS-AFM was carried out using a commercial AFM system (SPM-5500, Agilent) under a 5% H_2 atmosphere at temperatures between 30 and 70 °C and humidities between 0 and 70% RH (relative humidity). The gases were humidified by a bubbler set at desired temperature. The CS-AFM measurement at 30 °C and 40% RH was not able to be carried out due to the low bubbler temperature required, 14.9 °C. The morphological and current images were obtained at the contact mode with the contact force of 20 nN. For analyzing the current images, the threshold value was set at a background current of 0.4 pA.

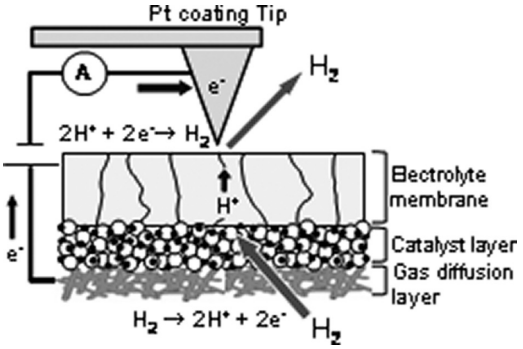

Figure 1. Schematic illustration of the principle of the current-sensing AFM measurement under hydrogen atmosphere.

dx.doi.org/10.1021/jp312041c | J. Phys. Chem. B 2013, 117, 3892−3899

3. RESULTS AND DISCUSSION

3.1. Proton Conductivity of SPE-bl-1 Membrane. The molecular structure of SPE-bl-1, its proton conductivity, and water uptake as a function of humidity are shown in Figure 2, a, b, and c, respectively. The proton conductivity of SPE-bl-1 membrane increased with increasing the humidity and temperature similarly to Nafion (see Supporting Information, Figure S1). In the low-humidity region, the water uptake showed little difference at different temperatures, while, at a higher humidity of 70% RH, exhibited a slight decrease from 20 to 17% upon raising the temperature from 40 to 80 °C. Nevertheless, with this temperature elevation at 70% RH, the proton conductivity was enhanced by 1.6 times. With the increase of humidity from 40 to 70% RH, the water uptake increased at each temperature by 1.5−1.6 times, accompanied by a noticeable increase of the proton conductivity by 5−6 times. Such properties of the SPE-bl-1 membrane will be later discussed in comparison with the CS-AFM observations.

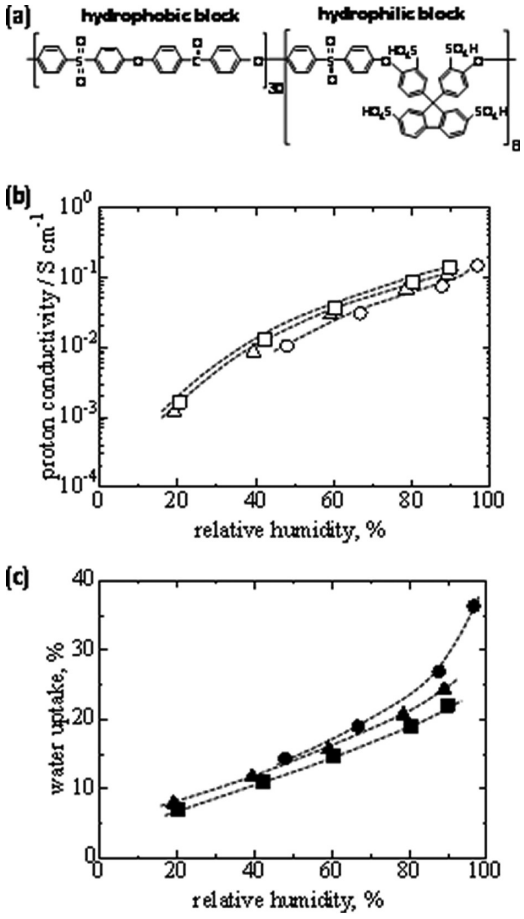

Figure 2. Chemical structure (a), proton conductivity (b), and water uptake (c) of an SPE-bl-1 membrane at (○,●) 40, (△,▲) 60, and (□,■) 80 °C.

Bulk and surface structures of SPE-bl-1 membrane were investigated by STEM and AFM, respectively. A cross-sectional STEM image of a lead-ion-exchanged SPE-bl-1 membrane is shown in Figure 3a. The lead-ion-exchanged sulfonic acid groups forming hydrophilic clusters are observed as dark domains. The size of the hydrophilic domains was 10 ± 3 nm and the ratio of the hydrophilic domains was approximately 30%. In contrast, hydrophobic regions were observed brightly

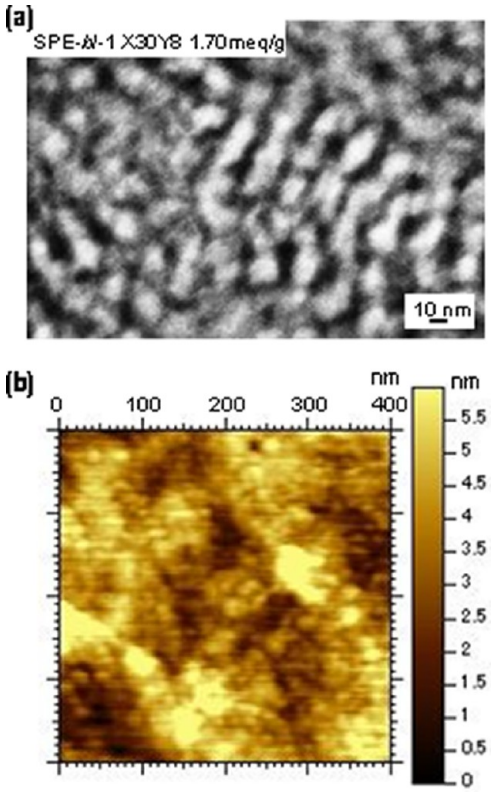

Figure 3. STEM image in vacuum at room temperature (a) and AFM topography at 70% RH and 30 °C (b) of an SPE-bl-1 membrane.

with a size of 11 ± 4 nm. Due to the higher concentration of sulfonic acid groups in the hydrophilic blocks, the phase separation of the SPE-bl-1 membrane was very uniform and enhanced compared to a random SPE copolymer membrane previously synthesized.[24] In comparison with the STEM observation carried out inside the dried samples under vacuum, AFM measurements were applied to analyzing the membrane surface under the humidified conditions. Figure 3b shows an AFM image of the surface of SPE-bl-1 membrane in an area of 400 nm × 400 nm at 30 °C and 70% RH. The surface was smooth with an average corrugation of 2−3 nm. The phase separation of hydrophobic and hydrophilic domains was not detectable in a contact mode. The morphology of the membrane surface did not change at different temperatures and humidities in our experimental conditions.

3.2. *I*−*V* Curves. Figure 4 shows the current versus bias voltage (*I*−*V*) obtained between the AFM tip and the GDE in an environment-controlling chamber after being purged with either air or 5% H_2 (gas flow rate = 100 mL min^{-1}) at 30 °C for 2 h. During the *I*−*V* measurements, the flow rate was reduced to 10 mL min^{-1} for all the gases. In the case in air, protons were produced by the electrolysis of water. Under hydrogen (Figure 1), similar to a hydrogen pump, protons were formed by the oxidation of hydrogen gas at the anode, transferred through the PEM, and reduced back to hydrogen at the cathode.

Under dry conditions, with either air or 5% H_2, almost no current was detected due to a low ionic conductivity and a decreased reaction activity. When the humidity was increased to 70% RH, currents were observed under both air and 5% H_2. Owing to the lower equivalent potential and lower over-potential for the oxidation/reduction reactions of hydrogen, the overall cell voltage in hydrogen was much lower than that in air.

dx.doi.org/10.1021/jp312041c | J. Phys. Chem. B 2013, 117, 3892−3899

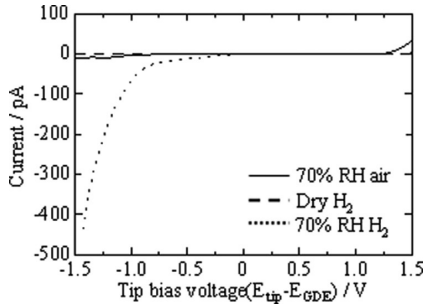

Figure 4. *I*−*V* curves obtained between an SPE-bl-1 membrane surface and a Pt−Ir-coated AFM tip at 30 °C under air at 70% RH (solid line), under 5% H_2 (N_2 balance) at 0% RH (dashed line), and under 5% H_2 at 70% RH (dotted line).

Under air, the current was observed at both negative and positive tip bias, but it was much smaller than those obtained under H_2 even at large bias voltages. In the case under H_2, an asymmetric *I*−*V* curve was observed, and a large current density was detected only at a negative tip bias. This may be due to an asymmetry of the electrode configuration in our electrochemical system, in which were used the GDE with a large Pt surface area (approximately 6 cm^2 per 1 mm^2 of GDE) and the Pt−Ir tip apex with an extremely small contact area (several nm^2). We assumed that the asymmetric *I*−*V* curves were explained by the smaller rate of the hydrogen oxidation reaction than that of the evolution reaction on the Pt surface. When Nafion was used for the *I*−*V* measurements (see Supporting Information, Figure S2), the tendency was similar, but the current was larger by approximately 10 times than that on SPE-bl-1. The increase in the proton-conducting current is not very steep in Figure 4 because of the diffusion of protons inside the membranes; the increase in current would become steeper with use of a thinner membrane.

3.3. CS-AFM Imaging of SPE-bl-1 Membrane at Various Relative Humidities and Temperatures. The CS-AFM image on a SPE-bl-1 surface, in an area of 1 μm × 1 μm under 5% H_2 at 30 °C and 70% RH, is shown in Figure 5. At bright proton-conductive areas, visualized as bright spots, where the current was detected, the hydrophilic regions inside the membrane must be effectively connected out to the surface. The dark areas, on the other hand, represent nonconductive or low-conductive regions. The proton-conductive spots were of about 10 nm in diameter. The proton-conductive spots were distributed rather inhomogeneously on the surface. The spot size on SPE-bl-1 was in agreement with that of the hydrophilic clusters observed in the STEM image (Figure 3a). A closer look at the CS-AFM image reveals that the proton-conducting spots had an ellipse shape in the horizontal scanning direction, probably due to the contact between the surface and the AFM tip. Therefore, the real diameter was taken as the size of the spot perpendicular to the scanning direction. The sizes obtained in this manner will be later used in the statistic analyses. By CS-AFM, morphological and current images were simultaneously obtained, whereas the correlation was hardly seen between the images.

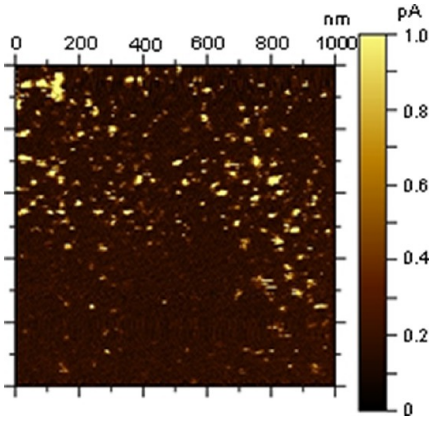

Figure 5. CS-AFM image on an SPE-bl-1 membrane under 5% H_2 (N_2 balance) at 30 °C and 70% RH. Tip bias voltage = −0.6 V.

By CS-AFM, the ratio of proton-conductive regions on the surface was obtained to be 5−10%. This value is much smaller than the value measured in the STEM images, 30% (Figure 3a); This difference can be explained by the fact that CS-AFM images reflect not the distribution of the hydrophilic clusters located on the membrane surface but the distribution of hydrophilic clusters connected to the active proton paths inside the membrane.

We have also carried out the CS-AFM measurements on a Nafion membrane surface under the same conditions (see Supporting Information, Figure S3). With our experimental setup, the current distribution on Nafion was detected very uniformly on the surface; in fact, individual proton-conducting spots were not distinguishable because the distance between the hydrophilic clusters was so close to each other, estimated to be less than a couple of nanometers, and the distribution was so uniform. The hydrophilic clusters of Nafion forming uniform proton-conducting networks must be contributing to the homogeneous proton transfer at the surface.

The CS-AFM measurements on the SPE-bl-1 membrane were carried out at various temperatures and relative humidities under 5% H_2. The CS-AFM images obtained at 30, 50, and 70 °C and 0, 40, and 70% RH are shown in Figure 6. These images are enlarged to 400 nm × 400 nm. Before the measurements, the chamber was maintained under the measurement conditions for more than 2 h. On the upper row at 0% RH, the proton-conductive areas were not observed due to a very low conductivity and/or limited connectivity of the hydrophilic network inside the membrane under the dry conditions. The CS-AFM image obtained at 40% RH showed some bright spots or proton-conducting spots on the membrane surface, indicating network structures of the hydrophilic domains. With increase of the relative humidity to 70%, the number of the spots increased, and the spots became brighter. On the other hand, little dependency on the temperature was observed in the CS-AFM images, consistent with the results on the proton conductivity measured by impedance spectroscopy (Figure 2b).

Figure 7 shows the histograms of the size of the proton-conducting spots observed by CS-AFM under different conditions. The size of the proton-conducting spots was almost constant, 10 ± 5 nm, when the temperature was changed, but by increasing humidity, the size and the size distribution became slightly larger and broadened, respectively. This average size is consistent with the hydrophilic domain observed in Figure 3a.

Figure 8, a and b, shows the total numbers of the proton-conducting spots and the percentages of the total conducting area, respectively, in the scanning area of 1 μm^2. The temperature and the humidity were the same as in Figure 6. The number of spots increased significantly at higher humidity,

dx.doi.org/10.1021/jp312041c | J. Phys. Chem. B 2013, 117, 3892−3899

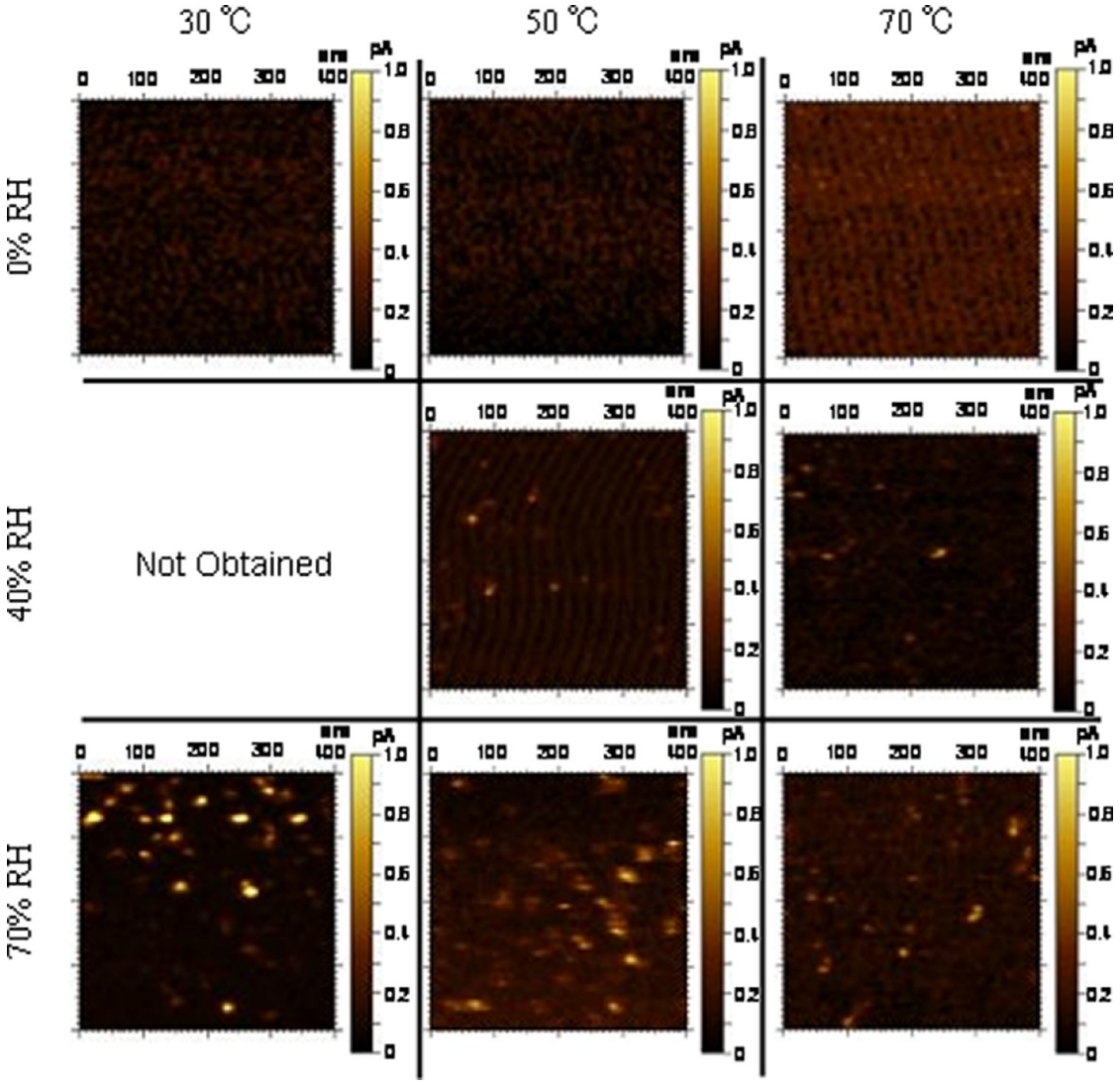

Figure 6. CS-AFM images of SPE-bl-1 membrane at 30−70 °C and 0−70% RH under 5% H_2. Tip bias voltage = −0.6 V. The image at 40% RH and 30 °C was not obtained due to experimental difficulty.

and the increase was larger at higher temperature, e.g., from 180 to 320 (a factor of 1.8) at 50 °C and from 90 to 540 (a factor of 6) at 70 °C with the humidity change from 40 to 70% RH. Even at 70 °C and 70% RH, the conducting area was less than 6% of the surface. In the case of Nafion, although the detected current changed under the different conditions, the distribution of the spots on the surface was always uniform (see Supporting Information, Figure S3). The decrease in the number of the proton-conducting spots at a lower humidity observed on the surface of SPE-bl-1 membrane should be due to the inefficiency of the proton network inside or at the surface of the membrane even though the hydrophobic/hydrophilic domains are uniformly established inside (Figure 3a). This inefficient proton network at low humidity could be a reason for the lower proton conductivity of SPE-bl-1 than of Nafion at low humidity.

The number and the area of the proton-conducting spots at 70 °C were counted smaller than those at 50 °C at a low humidity of 40% RH, as shown in Figure 8a,b. This dependency on the temperature at low humidity is not well-understood and should be studied in more detail in future studies.

Figure 9 shows bar graphs of a "pseudo current density" at various measurement conditions, which is defined as the integrated currents detected at the AFM tip at individual 256 × 256 points in one CS-AFM image, subsequently divided by the scanned area. The "pseudo current density", therefore, is not the actual current density but expected to be nearly proportional to the actual protonic current through the PEM or the proton conductivity. The pseudo current densities became larger by factors of 1.9 and 3.4 at 50 and 70 °C, respectively, by the increase of humidity from 40 to 70% RH. Based on the data in Figure 2, b and c, obtained by impedance spectroscopy, the conductivity increased by a factor of 5 (from 0.011 to 0.056 S cm^{-1}) at 70 °C when the humidity was changed from 40 to 70% RH. This mismatch between the pseudo current density obtained by CS-AFM and the conductivity measured by impedance spectroscopy could be explained by the differences in the two methods; the former involves the processes of hydrogen oxidation, proton transfer through the membrane, and hydrogen generation. Moreover, the former is the value along the PEM plane whereas the latter that through the membrane plane. These two methods are complementary.

In this paper, the CS-AFM under the controlled H_2 conditions was demonstrated to provide useful information

dx.doi.org/10.1021/jp312041c | J. Phys. Chem. B 2013, 117, 3892−3899

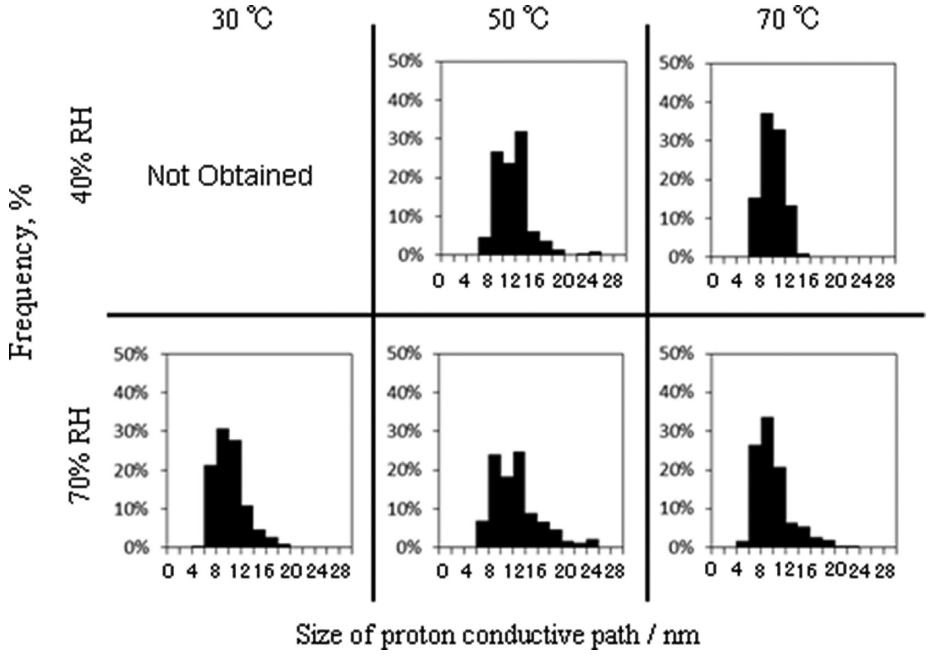

Figure 7. Size distribution histograms of the proton-conductive paths on SPE-bl-1 surface at various temperatures and humidities. The data at 40% RH and 30 °C is not shown due to experimental difficulty.

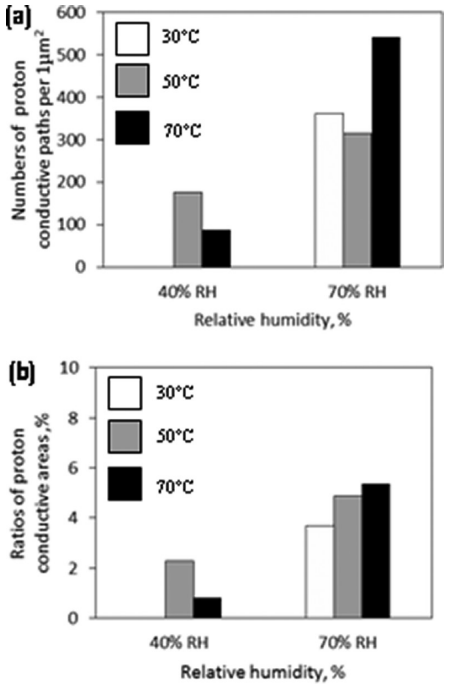

Figure 8. Number (a) and the area ratio (b) of the proton-conducting paths at various temperatures and humidities. The data at 40% RH and 30 °C is not shown due to experimental difficulty.

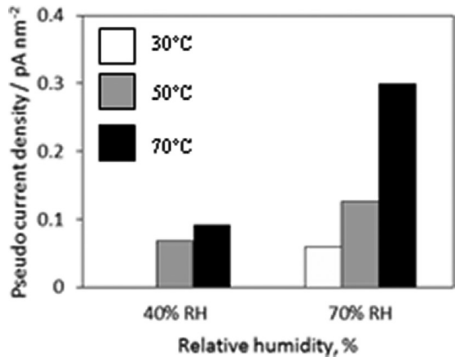

Figure 9. "Pseudo current density" at various temperatures and humidities. The data at 40% RH and 30 °C is not shown due to experimental difficulty.

for the designs of effective ionic conducting spots in a novel PEM under various humidities and temperatures, or the conditions for the practical PEFC operations. The proton-transfer mechanism has been still a controversial issue and requires a more detailed study. Furthermore, the effect of the phase-separated structure of the multiblock copolymers for the proton-transfer process in the membrane still remains as an arguable topic. To clarify these influences, the CS-AFM measurements on other PEMs with different structures, and under the true operation condition, where the HOR takes place at the anode and the ORR at the cathode, are attractive and important for future research.

4. CONCLUSIONS

For analyzing the proton-conductive spots on electrolyte membranes under the hydrogen atmosphere at different temperatures and humidities, we developed a novel CS-AFM system with an environment-controlling chamber. Using the system, the distribution of the proton-conductive spots, which were connected to the active proton-conductive paths inside the membrane, on the SPE-bl-1 surface was imaged and investigated. The average sizes of the proton-conducting spots remained nearly constant, 8−13 nm, regardless of the temperature and the humidity. The numbers of the spots at 50 °C in 1 μm^2 were 180 and 320 at 40 and 70% RH, respectively, and those at 70 °C were 90 and 540 at 40 and 70% RH, respectively. No proton-conducting paths were observed at 0% RH. The lower proton conductivity of SPE-bl-1 membrane than that of Nafion at low humidity could be explained by the

dx.doi.org/10.1021/jp312041c | J. Phys. Chem. B 2013, 117, 3892−3899

decrease in the number of the active paths possibly due to the insufficiency of the connectivity between neighboring hydrophilic clusters. In addition, the "pseudo current density" should imply the proton-transfer rates across the membrane under different conditions. To clarify the impact of the phase-separated structure on the fuel cell performance, we are planning to investigate the property of the proton-conducting paths on different multiblock copolymer PEMs.

■ ASSOCIATED CONTENT

Supporting Information

(S1) Proton conductivity and water uptake of Nafion. (S2) *I*–*V* curves obtained on Nafion with various thicknesses. (S3) CS-AFM image and cross-sectional current on Nafion. This material is available free of charge via the Internet at http://pubs.acs.org.

■ AUTHOR INFORMATION

Corresponding Author

*Tel./Fax: +81-55-254-7129 (J.I.); +81-55-254-7091 (M.W.). E-mail: jinukai@yamanashi.ac.jp (J.I.); m-watanabe@yamanashi.ac.jp (M.W.).

Present Address

[¶]Fuel Cell Research Center, Korea Institute of Energy Research, 152 Gajeong-ro, Yuseong, Daejeon, 305-343, Korea.

Notes

The authors declare no competing financial interest.

■ ACKNOWLEDGMENTS

This work was supported by the "Research on Nanotechnology for High Performance Fuel Cells (HiPer-FC)" project from the New Energy and Industrial Technology Development Organization (NEDO) of Japan.

■ REFERENCES

(1) Carrette, L.; Friedrich, K. A.; Stimming, U. Fuel Cells–Fundamentals and Applications. *Fuel Cells* **2001**, *1*, 5–39.

(2) Hickner, M. A.; Pivovar, B. S. The Chemical and Structural Nature of Proton Exchange Membrane Fuel Cell Properties. *Fuel Cells* **2005**, *5*, 213–229.

(3) Peighambardoust, S. J.; Rowshanzamir, S.; Amjadi, M. Review of the proton exchange membranes for fuel cell applications. *Int. J. Hydrogen Energy* **2010**, *35*, 9349–9384.

(4) Kerres, J.; Cui, W.; Reichle, S. New sulfonated engineering polymers via the metalation route. I. Sulfonated poly(ethersulfone) PSU Udel via metalation-sulfination-oxidation. *J. Polym. Sci., Part A: Polym. Chem.* **1996**, *34*, 2421–2438.

(5) Kobayashi, T.; Rikukawa, M.; Sanui, K.; Ogata, N. Proton-conducting polymers derived from poly(ether-etherketone) and poly(4-phenoxybenzoyl-1,4-phenylene). *Solid State Ionics* **1998**, *106*, 219–225.

(6) Wang, F.; Hickner, M.; Kim, Y. S.; Zawodzinski, T. A.; McGrath, J. E. Direct polymerization of sulfonated poly(arylene ether sulfone) random (statistical) copolymers: candidates for new proton exchange membranes. *J. Membr. Sci.* **2002**, *197*, 231–242.

(7) Fang, J.; Guo, X.; Harada, S.; Watari, T.; Tanaka, K.; Kita, H.; Okamoto, K. Novel Sulfonated Polyimides as Polyelectrolytes for Fuel Cell Application. 1. Synthesis, Proton Conductivity, and Water Stability of Polyimides from 4,4′-Diaminodiphenyl Ether-2,2′-disulfonic Acid. *Macromolecules* **2002**, *35*, 9022–9028.

(8) Bae, J.-M.; Honma, I.; Murata, M.; Yamamoto, T.; Rikukawa, M.; Ogata, N. Properties of selected sulfonated polymers as proton-conducting electrolytes for polymer electrolyte fuel cells. *Solid State Ionics* **2002**, *147*, 189–194.

(9) Miyatake, K.; Chikashige, Y.; Watanabe, M. Novel Sulfonated Poly(arylene ether): A Proton Conductive Polymer Electrolyte Designed for Fuel Cells. *Macromolecules* **2003**, *36*, 9691–9693.

(10) Hickner, M. A.; Ghassemi, H.; Kim, Y.-S.; Einsla, B. R.; McGrath, J. E. Alternative Polymer Systems for Proton Exchange Membranes (PEMs). *Chem. Rev.* **2004**, *104*, 4587–4612.

(11) Xing, P.; Robertson, G. P.; Guiver, M. D.; Mikhailenko, S. D.; Kaliaguine, S. Sulfonated poly(aryl ether ketone)s containing naphthalene moieties obtained by direct copolymerization as novel polymers for proton exchange membranes. *J. Polym. Sci., Part A: Polym. Chem.* **2004**, *42*, 2866–2876.

(12) Gil, M.; Ji, X.; Li, X.; Na, H.; Hampsey, J. E.; Lu, Y. Direct synthesis of sulfonated aromatic poly(ether ether ketone) proton exchange membranes for fuel cell applications. *J. Membr. Sci.* **2004**, *234*, 75–81.

(13) Einsla, B. R.; Hong, Y.-T.; Kim, Y. S.; Wang, F.; Gunduz, N.; McGrath, J. E. Sulfonated naphthalene dianhydride based polyimide copolymers for proton-exchange-membrane fuel cells. I. Monomer and copolymer synthesis. *J. Polym. Sci., Part A: Polym. Chem.* **2004**, *42*, 862–874.

(14) Smitha, B.; Sridhar, S.; Khan, A. A. Solid polymer electrolyte membranes for fuel cell applications—a review. *J. Membr. Sci.* **2005**, *259*, 10–26.

(15) Yasuda, T.; Li, Y.; Miyatake, K.; Hirai, M.; Nanasawa, M.; Watanabe, M. Synthesis and properties of polyimides bearing acid groups on long pendant aliphatic chains. *J. Polym. Sci., Part A: Polym. Chem.* **2006**, *44*, 3995–4005.

(16) Kim, D. S.; Robertson, G. P.; Guiver, M. D.; Lee, Y. M. Synthesis of highly fluorinated poly(arylene ether)s copolymers for proton exchange membrane materials. *J. Membr. Sci.* **2006**, *281*, 111–120.

(17) Tian, S. H.; Shu, D.; Wang, S. J.; Xiao, M.; Meng, Y. Z. Poly(Arylene Ether)s with Sulfonic Acid Groups on the Backbone and Pendant for Proton Exchange Membranes Used in PEMFC Applications. *Fuel Cells* **2007**, *7*, 232–237.

(18) Schuster, M.; Kreuer, K.-D.; Andersen, H. T.; Maier, J. Sulfonated Poly(phenylene sulfone) Polymers as Hydrolytically and Thermooxidatively Stable Proton Conducting Ionomers. *Macromolecules* **2007**, *40*, 598–607.

(19) Kerres, J.; Ullrich, A.; Meier, F.; Häring, T. Synthesis and characterization of novel acid–base polymer blends for application in membrane fuel cells. *Solid State Ionics* **1999**, *125*, 243–249.

(20) Kim, Y. S.; Sumner, M. J.; Harrison, W. L.; Riffle, J. S.; McGrath, J. E.; Pivovar, B. S. Direct Methanol Fuel Cell Performance of Disulfonated Poly(arylene ether benzonitrile) Copolymers. *J. Electrochem. Soc.* **2004**, *151*, A2150–A2156.

(21) Asano, N.; Aoki, M.; Suzuki, S.; Miyatake, K.; Uchida, H.; Watanabe, M. Aliphatic/Aromatic Polyimide Ionomers as a Proton Conductive Membrane for Fuel Cell Applications. *J. Am. Chem. Soc.* **2006**, *128*, 1762–1769.

(22) Miyatake, K.; Chikashige, Y.; Higuchi, E.; Watanabe, M. Tuned Polymer Electrolyte Membranes Based on Aromatic Polyethers for Fuel Cell Applications. *J. Am. Chem. Soc.* **2007**, *129*, 3879–3887.

(23) Bae, B.; Miyatake, K.; Watanabe, M. Sulfonated poly(arylene ether sulfone) ionomers containing fluorenyl groups for fuel cell applications. *J. Membr. Sci.* **2008**, *310*, 110–118.

(24) Bae, B.; Miyatake, K.; Watanabe, M. Synthesis and Properties of Sulfonated Block Copolymers Having Fluorenyl Groups for Fuel-Cell Applications. *ACS Appl. Mater. Interfaces* **2009**, *1*, 1279–1286.

(25) Bae, B.; Miyatake, K.; Watanabe, M. Sulfonated Poly(arylene ether sulfone ketone) Multiblock Copolymers with Highly Sulfonated Block. Synthesis and Properties. *Macromolecules* **2010**, *43*, 2684–2691.

(26) Bae, B.; Hoshi, T.; Miyatake, K.; Watanabe, M. Sulfonated Block Poly(arylene ether sulfone) Membranes for Fuel Cell Applications via Oligomeric Sulfonation. *Macromolecules* **2011**, *44*, 3884–3892.

(27) Bae, B.; Yoda, T.; Miyatake, K.; Uchida, H.; Watanabe, M. Proton-Conductive Aromatic Ionomers Containing Highly Sulfonated Blocks for High-Temperature-Operable Fuel Cells. *Angew. Chem., Int. Ed.* **2010**, *49*, 317–320.

(28) Bae, B.; Yoda, T.; Miyatake, K.; Uchida, M.; Uchida, H.; Watanabe, M. Sulfonated Poly(arylene ether sulfone ketone) Multiblock Copolymers with Highly Sulfonated Block. Fuel Cell Performance. *J. Phys. Chem. B* **2010**, *114*, 10481−10487.
(29) Hsu, W. Y.; Gierke, T. D. Ion transport and clustering in nafion perfluorinated membranes. *J. Membr. Sci.* **1983**, *13*, 307−326.
(30) Schmidt-Rohr, K.; Chen, Q. Parallel cylindrical water nanochannels in Nafion fuel-cell membranes. *Nat. Mater.* **2008**, *7*, 75−83.
(31) Liu, Y.; He, J.; Kwon, O.; Zhu, D.-M. Probing local surface conductance using current sensing atomic force microscopy. *Rev. Sci. Instrum.* **2012**, *83*, 013701.
(32) Bussian, D. A.; O'Dea, J. R.; Metiu, H.; Buratto, S. K. Nanoscale Current Imaging of the Conducting Channels in Proton Exchange Membrane Fuel Cells. *Nanolett.* **2007**, *7*, 227−232.
(33) Xie, X.; Kwon, O.; Da-Ming, Z.; Nguyen, T. V.; Liu, G. J. Local Probe and Conduction Distribution of Proton Exchange Membranes. *J. Phys. Chem. B* **2007**, *111*, 6134−6140.
(34) Aleksandrova, E.; Hiesgen, R.; Friedrich, K. A.; Roduner, E. Electrochemical atomic force microscopy study of proton conductivity in a Nafion membrane. *Phys. Chem. Chem. Phys.* **2007**, *9*, 2735−2743.
(35) Aleksandrova, E.; Hiesgen, R.; Friedrich, K. A.; Roduner, E. Proton Conductivity Study of a Fuel Cell Membrane with Nanoscale Resolution. *Chem. Phys. Chem.* **2007**, *8*, 519−522.
(36) Takimoto, N.; Ohira, A.; Takeoka, Y.; Rikukawa, M. Surface Morphology and Proton Conduction Imaging of Nafion Membrane. *Chem. Lett.* **2008**, *37*, 164−165.
(37) Kang, Y.; Kwon, O.; Xie, X.; Zhu, D.-M. Conductance Mapping of Proton Exchange Membranes by Current Sensing Atomic Force Microscopy. *J. Phys. Chem. B* **2009**, *113*, 15040−15046.
(38) Hiesgen, R.; Aleksandrova, E.; Meichsner, G.; Wehl, I.; Rodunder, E.; Friedrich, K. A. High-resolution imaging of ion conductivity of Nafion® membranes with electrochemical atomic force microscopy. *Electrochim. Acta* **2009**, *55*, 423−429.
(39) Sanchez, D. G.; Diaz, D. G.; Hiesgen, R.; Wehl, I.; Friedrich, K. A. Oscillations of PEM fuel cells at low cathode humidification. *J. Electroanal. Chem.* **2010**, *649*, 219−231.
(40) Kwon, O.; Kamg, Y.; Wu, S.; Zhu, D.-M. Characteristics of Microscopic Proton Current Flow Distributions in Fresh and Aged Nafion Membranes. *J. Phys. Chem. B* **2010**, *114*, 5365−5370.
(41) Kwon, O.; Wu, S.; Zhu, D.-M. Configuration Changes of Conducting Channel Network in Nafion Membranes due to Thermal Annealing. *J. Phys. Chem. B* **2010**, *114*, 14989−14994.
(42) Kwon, O.; Kamg, Y.; Wu, S.; Zhu, D.-M. Characterization of Proton Conduction in Nafion Membranes Using Current Sensing Atomic Force Microscopy. *ECS Trans.* **2010**, *33*, 1035−1044.
(43) He, Q.; Kusoglu, A.; Lucas, I. T.; Clark, K.; Weber, A. Z.; Kostecki, R. Correlating Humidity-Dependent Ionically Conductive Surface Area with Transport Phenomena in Proton-Exchange Membranes. *J. Phys. Chem. B* **2011**, *115*, 11650−11657.
(44) Aleksandrova, E.; Hink, S.; Hiesgen, R.; Rodunder, E. Spatial distribution and dynamics of proton conductivity in fuel cell membranes: potential and limitations of electrochemical atomic force microscopy measurements. *J. Phys.: Condens. Matter* **2011**, *23*, 234109.
(45) Takimoto, N.; Takamuku, S.; Abe, M.; Ohira, A.; Lee, H.-S.; McGrath, J. E. Conductive area ratio of multiblock copolymer electrolyte membranes evaluated by e-AFM and its impact on fuel cell performance. *J. Power Sources* **2009**, *194*, 662−666.
(46) Hink, S.; Aleksandrova, E.; Rodunder, E. Electrochemical AFM Investigations of Proton Conducting Membranes. *ECS Trans.* **2010**, *33*, 57−70.
(47) Song, J. M.; Uchida, H.; Watanabe, M. Effect of Wet-Proofing Treatment of Carbon Backing Layer in Gas Diffusion Electrodes on the PEFC Performance. *Electrochemistry* **2005**, *73*, 189−193.
(48) Aoki, M.; Asano, N.; Miyatake, K.; Uchida, H.; Watanabe, M. Durability of Sulfonated Polyimide Membrane Evaluated by Long-Term Polymer Electrolyte Fuel Cell Operation. *J. Electrochem. Soc.* **2006**, *153*, A1154−A1158.
(49) Lin, C.-C.; Lien, W.-F.; Wang, Y.-Z.; Shiu, H.-W.; Lee, C.-H. Preparation and performance of sulfonated polyimide/Nafion multilayer membrane for proton exchange membrane fuel cell. *J. Power Sources* **2012**, *200*, 1−7.